Retrospective Theses and Dissertations

Iowa State University Capstones, Theses and Dissertations

2007

Titanium dioxide particle size effects on the degradation of organic molecules

Timothy Lee Hathway
Iowa State University

Titanium dioxide particle size effects on the degradation of organic molecules

by

Timothy Lee Hathway

A thesis submitted to the graduate faculty

in partial fulfillment of the requirements for the degree of

MASTER OF SCIENCE

Major: Chemistry (Organic Chemistry)

Program of Study Committee:
William Jenks, Major Professor
Richard Larock
Hans Stauffer

Iowa State University

Ames, Iowa

2007

UMI Number: 1447547

UMI®

UMI Microform 1447547

www.manaraa.com

TABLE OF CONTENTS

CHAPTER 1

General Introduction

1.1. Introduction

The cleanup of wastewater and air pollution has become increasingly important in the past decades, and burgeoning populations require more and more energy and resources to sustain a comfortable standard of living. Two major types of pollution can be identified that encompass all others: technological and agricultural. Technological pollution is that produced from human sources: industrial, military, etc. Compounds with low solubility in water characterize this type of pollution. A separate layer forms on the surface that negatively affects the physical properties of the water (oxygen uptake, surface tension), and also hampers any living thing that comes in contact with the surface. The second major type of pollution is that of high concentrations of nutrients that leach into the soil and drain into water sources mainly from agriculture. The most notable effect of this form of pollution is the overgrowth of algae and other plants in the water source that cannot be removed by natural means, which build up in and prematurely age a water source.[1] With these issues in mind, freshwater sources are of particular concern as they are the major source of drinking water for the world's population. Runoff from pollution sources enters bodies of water not naturally able to contain and remediate them.[2] Although the prevention of pollution is critical to cleanup efforts, repairing the current damage is a great concern.

Many different types of chemicals enter ground and surface water sources, both inorganic and organic. Heavy metals, nitrates, and organometallics (especially tin compounds) are the most common inorganic sources of pollution, both technologically and agriculturally based.[3] Some of the most common and harmful organic pollutants in wastewater and other polluted sources are organic molecules, including polychlorinated biphenyls (PCBs), chlorinated and brominated phenols, chlorinated hydrocarbons, atrazines, surfactants, and a plethora of aromatics contained in pesticide runoff, sewage, and industrial sources.[3] Although this is by no means an exhaustive list, it does highlight the fact that many of these are small molecules that are at least mildly soluble in water sources and are toxic to all forms of life. Physical means of removing waste include filtration, distillation, ion exchange, and reverse osmosis. Most of these methods, though, are useful only for insoluble or inorganic compounds.[1] Chemical methods for removal of organics include waste incineration, anaerobic digestion, and physicochemical methods. Chemical oxidation is a physicochemical method involving highly oxidizing materials used to convert organic pollutants to carbon dioxide, water, and other fully oxidized species like nitrates and sulfates. By oxidative means, harmful organic compounds can be broken down into substances that the other methods (ion exchange, distillation) can easily separate from water.

These chemical oxidation processes can be divided into two major classes: conventional and advanced. Conventional processes[4] involve wet chemical oxidizing agents, including ozone, persulfate, and Fenton reagents (Fe^{3+}/H_2O_2). These methods have been proven effective in the remediation of a wide array of organics, but have several disadvantages. These include toxicity and potential safety hazards of the strong

oxidizing agents (like H_2O_2 or permanganate). Also their high reactivity can lead to a short lifetime and thus incomplete oxidation of organics, producing intermediates that may be more toxic than the original pollutant.[4]

A heavily studied alternative to conventional oxidation is that of advanced oxidation using sonolysis, radiolysis, or photolysis. Advanced oxidation processes (AOPs) are those processes that involve the creation of *in situ* oxidants with high oxidation potentials.[5] Of particular interest is photolysis, known as photodegradation, in terms of waste treatment. The most widely employed light-assisted remediation methods are direct photolysis, degradation with UV/H_2O_2, photolysis with ozone, and photocatalysis.[6]

As many organic compounds are resistant to direct photolysis under visible or UV light, a sensitizer or photocatalyst must be employed. Solution phase UV reagents, like H_2O_2, have many of the same downfalls that non-AOP chemical oxidizers have, including the tendency to react completely before the intended pollutant is sufficiently destroyed. Photocatalysts, being generally water-insoluble, do not suffer from this limitation, as many are rugged under aqueous conditions and resistant to photochemical degradation. Both of these methods generate hydroxyl radicals and other strongly oxidizing species in solution.[5] Therefore, photocatalysis and homogenous photodegradation share many of the same mechanistic traits, including an exceptional ability to degrade organic molecules to fully oxidized forms, as shown in Reaction 1.

$$C_xH_{2x} + xO_2 \xrightarrow[h\nu]{TiO_2} xCO_2 + \frac{x}{2}H_2O$$
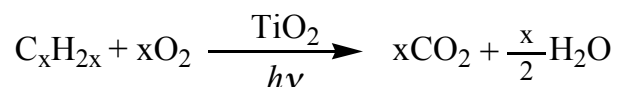
Reaction 1. Destruction of a generic organic molecule using titanium dioxide and light

Semiconductor photocatalysis relies on the use of metal oxides to create oxidized holes, which directly react with adsorbed molecules. This subject is explained in further detail in section 1.3. In particular, titanium dioxide (TiO_2) has emerged as the most studied of these photocatalysts for its high degradation efficiency with almost any organic molecule and many other attractive properties, including physical and chemical stability and low price.[7]

Although many of the degradation characteristics of TiO_2 are known, many of the initial chemical processes of degradation that occur directly after excitation are still unclear. This thesis describes a study of the mechanistic organic chemistry occurring in the initial stages of the oxidative degradation of organic molecules at the surface of titanium dioxide photocatalysts. Specifically, the present studies focus on the effect of catalyst particle size on the degradation mechanism of organic molecules at various pH values. Also, organic molecules with well-defined oxidation chemistry are required in order to effectively study degradation mechanisms. Work is described in which two probe molecules are characterized for use in this research.

1.2. Thesis Organization

This thesis is divided into three chapters. Chapter 1 is a general introduction to the subject of water remediation and chemical oxidation. It explains the background information needed to understand the chemistry behind photocatalysis, with titanium dioxide as the subject of interest. The properties of titania in terms of its ability to degrade organic molecules are discussed.

Chapter 2 describes the effects of titania particle size on the degradation of ANP and 4-methoxyresorcinol (MRC). These two probe molecules yield degradation chemistry that has been well studied in order to ascertain mechanism based on product ratios. Nanometer scale titanium dioxide has shown the highest activity for the degradation of organic pollutants, but an optimum size has yet to be reached with an optimum charge carrier recombination to surface area ratio. To attain this, the Millennium PC catalyst series is studied and compared to a known catalyst, Degussa P25. The PC series are differentiated by size based on the extent of sintering performed. Each catalyst in the series is produced using the same procedure, with only the final sintering step varied by the amount of time spent annealing. This method produces catalysts that differ by particle size and surface area.
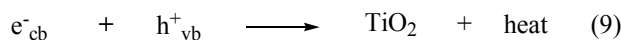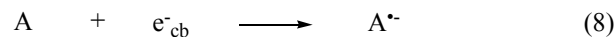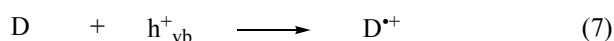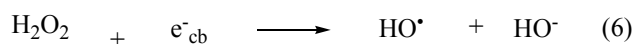
1.3. Semiconductor Photocatalysis

Semiconductors used for the photosensitization of organic molecules are usually metal oxides or metal sulfides. The most commonly studied semiconductors include

TiO_2, ZnO, WO_3, Fe_2O_3, and ZnS.[8] In searching for an ideal photocatalyst for remediation of organic molecules using sunlight, several factors must be taken into account; chief among them are oxidation potential and band gap energy. The oxidation potential is important, since the ability to form a photogenerated valence band hole (h^+_{vb}) or create a hydroxyl radical ($HO^\bullet_{ads}$) in water is key to its use as a photocatalyst for the oxidation of organic molecules. This is also true of the reducing power of the excited conduction band electron (e^-_{cb}), which must be of sufficient energy to reduce molecular oxygen to superoxide.[6] These two chemical processes are the key to the photocatalysis of organic molecules to harmless gaseous products (H_2O, CO_2) and inorganic ions (NO_3^-, SO_4^{2-}).

The band gap energy of the semiconductor defines the wavelength of light needed to excite the electron to the conduction band, which leaves a positively charged hole in the valence band, h^+_{vb}.[9] If the required wavelength is higher than the range of the solar spectrum (i.e. higher energy than that of solar output) for a given semiconductor to form charge carriers, then that semiconductor is of no use for the degradation of organics using sunlight without significant electronic modification. Titanium dioxide (TiO_2) has both a high oxidation potential and a band gap that allows for absorption of the UV portion of sunlight. Unfortunately, the UV portion makes up only about five percent of the solar emission spectrum.[7]
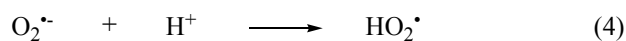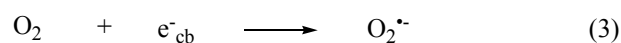
Despite the low solar absorbance, titania is considered the best choice for general photocatalytic needs as it fits other desirable criteria. TiO_2 is cheap, nontoxic, photolytically and chemically stable, and reusable with a high turnover rate. It is also easy to modify the chemical and physical characteristics of TiO_2, including absorption

range and particle size, which can be considered the most important means of modification of titania's oxidation capabilities. Methods of electronic modification of TiO_2 to extend the band gap to higher wavelengths will be discussed later.

$$TiO_2 \ + \ h\nu \ \longrightarrow \ e^-_{cb} \ + \ h^+_{vb} \quad (1)$$

$$H_2O_{ads} \ + \ h^+_{vb} \ \longrightarrow \ HO^{\bullet}_{ads} \ + \ H^+ \quad (2)$$

$$O_2 \ + \ e^-_{cb} \ \longrightarrow \ O_2^{\bullet-} \quad (3)$$

$$O_2^{\bullet-} \ + \ H^+ \ \longrightarrow \ HO_2^{\bullet} \quad (4)$$

$$HO_2^{\bullet} \ + \ HO_2^{\bullet} \ \longrightarrow \ H_2O_2 \ + \ O_2 \quad (5)$$

$$H_2O_2 \ + \ e^-_{cb} \ \longrightarrow \ HO^{\bullet} \ + \ HO^- \quad (6)$$

$$D \ + \ h^+_{vb} \ \longrightarrow \ D^{\bullet+} \quad (7)$$

$$A \ + \ e^-_{cb} \ \longrightarrow \ A^{\bullet-} \quad (8)$$

$$e^-_{cb} \ + \ h^+_{vb} \ \longrightarrow \ TiO_2 \ + \ heat \quad (9)$$
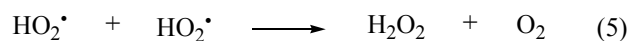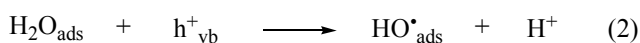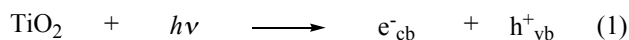
The chemical mechanism of titanium dioxide photocatalysis in water is shown in Equations 1-9. Figure 1 serves to show a pictorial representation of these processes. Equation 1 shows the initial reaction of titanium dioxide with light, producing a hole and an electron that act as the active excited species, which then react with water and oxygen as shown in equations 2-5. In aqueous conditions, Ti-OH groups are abundant and are the major source of hydroxyl radicals on the TiO_2 surface.[10] The downstream products of reactions with molecular oxygen are superoxide ($O_2^{\bullet-}$, Eq. 3) and often hydroxyl radical ($HO^{\bullet}$, Eq. 5), which can react with a nearby organic molecule. Equations 5 and 6 show the formation of hydrogen peroxide, which is known to split into two hydroxyl radicals in aqueous photolysis or to accept electrons as in equation 6.[11] The hole, h^+_{vb}, can also react

directly with an adsorbed organic donor (**D**) as in equation 7. In systems where TiO_2 is used to reduce molecules, as in a dye-sensitized solar cell, **A** is the organic molecule and **D** (Eq. 7) is a hole trap.[12] Equation 8 describes the reduction of an adsorbed molecule by the conduction band hole. In this case, **A** is considered an adsorbed molecule that can accept electrons. Reductive titanium dioxide chemistry is less studied due to the lower reducing power of e^-_{cb} compared to the high oxidizing power of h^+_{vb}.[8] Finally, equation 9 describes the recombination of the two charge carriers that releases heat. This process is known to occur for approximately ninety percent of all charge carriers formed, and is thus the major competing reaction with all "useful" chemistry in this system.
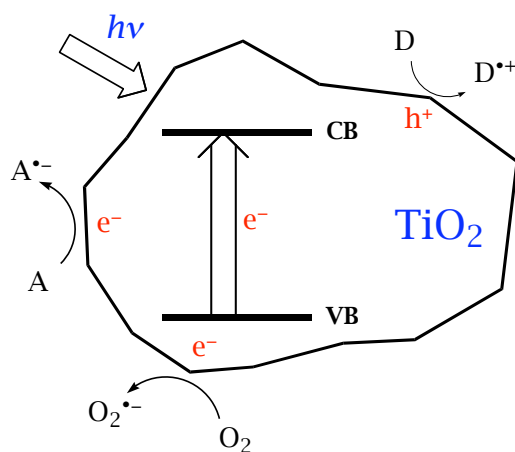
Figure 1. Pictorial view of TiO_2 excitation

A great deal of work has been carried out to understand surface recombination and many modifications of titania are based on reducing recombination.[13] The constant addition of an oxidizing agent to a reaction is required; otherwise, Equation 9 becomes the primary surface reaction since the charge carriers are not physically separated. A

common oxidant is molecular oxygen (O_2, Equation 8), which is added to titania

reactions since it acts as a stoichiometric oxidant (Reaction 1).[3] Due to its high reduction

potential and also the fact that the superoxide ion produced reacts further to produce more

hydroxyl radicals (Equations 3-5), O_2 makes an ideal trap for surface e^-_{cb}. O_2 is a better

electron acceptor than most organic molecules studied in this chemistry; thus equation 3

becomes an important process in aqueous photocatalysis.

Titanium dioxide exists in three crystalline phases: anatase, rutile, and brookite.

Of the three, brookite is the only photochemically inactive one, and is unimportant in the

field of photocatalysis from a reactivity standpoint. The synthesis of titanium dioxide

from well-known precursors can result in the formation of brookite, but careful control of

pH and temperature will eliminate the brookite crystallization.[14] On this note, the

synthesis of titanium dioxide at low temperatures can also yield an amorphous catalyst

that has been studied recently for photocatalytic activity, but was found to be well below

the threshold of rutile and anatase in terms of reactivity.[15]

Rutile was the first morphology to be studied in detail and thus much of the early

experimental and theoretical work on TiO_2 was based on it.[16,17] Rutile is the more

thermodynamically stable of the two photochemically active phases. Having a band gap

energy of 3.0 eV (418 nm), rutile would seem more ideal than anatase (3.2 eV, 387 nm),

but as studies have shown, it is actually weaker compared to anatase in the degradation of

many organic molecules,[7] which is most likely due to the more tightly packed crystal

structure in rutile, which has fewer defect sites in the bulk to trap photoexcited holes and

electrons and thus reduce charge carrier recombination. Most of the research on

remediation chemistry in the past few years has been performed on the anatase phase. Its

high band gap energy leads to a higher reduction potential, which allows for the oxidation of less reactive organic materials, like substituted benzenes. This, however, has the disadvantage of shifting the absorption band of the anatase catalyst to the blue, which allows for less sunlight absorption.

Modifications to the electronic structure of titanium dioxide in order to shift the absorption into the visible range are under intense study in the photocatalysis field. The most common types of alterations include pure titania modifications and doping with other elements or semiconductors. Pure titania variations involve changing the morphology and surface area (particle size). In terms of morphology, having both active crystal phases present makes a large difference in photocatalytic activity. Degussa P25 is a catalyst that contains 80% anatase and 20% rutile prepared by high temperature sintering.[18] When compared to the overwhelming majority of single-phase catalysts, P25 performs better in terms of degradation efficiency. This heightened photocatalytic activity has been attributed to the ability of excited electrons from the surface of anatase to become trapped in the lattice of the rutile phase, minimizing charge carrier recombination.[19]

The optimal particle size (and thus surface area) of titania has been studied by many groups over the years and affects both the amount of pollutants that can adsorb to the surface and the amount of charge carrier recombination that can occur, since recombination is a surface process.[20-22] Particle size considerations are discussed in further detail in chapter 3. In general, nanoscale titanium dioxide (1-100 nm) is considered to be the most active in the degradation of organic compounds, although many

micrometer scale catalysts are available and moderately effective. For reference, P25 has been measured to have a particle size of 25-35 nm.[18]

Other morphological modifications include the coating of titanium dioxide onto the surfaces of polymers and silica of multiple sizes and shapes for use in realistic water and air treatment. In addition, mesoporous TiO_2 and zeolites embedded with titania have been employed in efforts to dramatically increase surface area and allow for selective oxidations (i.e. chemical synthesis applications).[23]

The doping of titanium dioxide is a quickly progressing field where all manner of metals, non-metals, and other metal oxides have been coated onto or co-produced with titania crystallites in the interest of improving visible light absorption and/or decreasing recombination. One of the first and most successful doping strategies is the deposition of noble metals (like Pt or Au) onto the titanium dioxide surface, with the goal of splitting water into H_2 and O_2, which cannot be performed on naked TiO_2. When small (~2 nm) particles of Pt are deposited on the titania surface, an increase in the production of H_2 from adsorbed water molecules is observed.[7,24] This is due to the movement of electrons from the TiO_2 surface to the metal, which reduces the H_2O to H_2. In most cases, the deposition of noble metals is used for H_2 production as opposed to water purification. It should also be noted that the photoactivity of the rutile phase is greatly increased (for H_2 production) by the deposition of noble metals, especially platinum.[15] Unfortunately, noble metals are too expensive to utilize on a large scale. The use of transition metals, including Fe and Cr, as dopants has been performed, but in many cases these metals act as electron and hole traps, and adversely increase the recombination rate instead of lowering it.[13]

Titania has also been prepared as a homogenous mixture with other metal oxides, including SnO_2 and WO_3.[25] Tungstate doping in particular has been shown to shift the band gap of TiO_2 closer to the visible spectrum (2.86 eV vs. 3.21 eV for pure anatase).[26] This result is highly encouraging, as mentioned before, since increasing the sunlight absorption is one of the major goals of titania research. Increased degradative ability (i.e. rate of oxidation of organic molecules) is also reported for many of these catalysts compared to pure anatase and P25. This has been attributed to both increased surface acidity[27] of the mixed catalyst surface, as well as charge carrier trapping,[28] much like noble metal doping.

The most recent form of titania doping employs main group elements, especially C, S, and N. These elements substitute for O or Ti atoms in the titania lattice and introduce mid-gap levels in the electronic band structure where lower energy (and thus longer wavelength) excitations could occur, thus extending the band gap into the visible region, much like the case of tungstate doping.[13,26]

1.4. Degradation of Organic Molecules with TiO_2

Reaction 1 shows the general degradation of organic compounds with titanium dioxide. Much of the oxidative chemistry of titania is attributed to the action of highly oxidizing species like surface-adsorbed hydroxyl radical, $HO^{\bullet}_{ads}$, which are formed *in situ* in aqueous photolyses of titania. The mechanism of organic pollutant degradation is highly dependent on reaction conditions and the structure of the organic molecule. For the most part, the titania surface acts as an adsorption center for organic molecules, which

bind to it specifically or on an ad-layer within a few angstroms of the surface. From here, the molecule is oxidized, either by direct single electron transfer or by addition of $HO^{\bullet}_{ads}$. After this, a cascade of radical reactions ensue involving oxidation to CO_2 and H_2O or to an intermediate species. In a few isolated cases, recalcitrant species are formed that cannot be degraded further by TiO_2 (see below).[3]

To give a more specific example of the mechanism of degradation, the case of 4-chlorophenol (4CP) will be discussed. 4CP has been used extensively in mechanistic research as a model for a halogenated aromatic molecule.[29,30] This class of molecules is ubiquitous in terms of being found in polluted waters of many sources. In particular, 4CP has a set of photocatalytic products that can be confidently assigned to the action of certain oxidative processes. These include hydroxylation of the aromatic ring either directly or by *ipso* substitution of the chloro group, both of which are attributed to $HO^{\bullet}_{ads}$ chemistry.[29,30]

The other major process in the degradation of 4CP is opening of the aromatic ring, which is attributed to chemistry initiated by direct electron transfer from the aromatic ring to the titania surface.[31] This type of single electron transfer (SET) to the titania surface is thought to occur alongside hydroxyl radical chemistry, although due to the requirement of specific binding (for efficient electron transfer), it can be largely disfavored in the degradation of some molecules. In the case of phenols and especially catechols (1,2-benzenediols), SET chemistry manifests itself by the formation of ring-opened products where molecular oxygen has attacked the adsorbed molecule and two carboxylic acid groups are formed through a proposed dioxetane intermediate.[30] This matter will be discussed in detail in Chapter 3.

It has been stated multiple times that titania degrades almost any compound that it comes into contact with. However, there are exceptions, most notably cyanuric acid (Figure 2), which is the ultimate degradation product of a wide variety of triazines.[32,33] Although compounds like triazines are isolated cases, the phenomenon of incomplete degradation is very important as it can lead to insights into the chemical mechanisms governing the degradation of the molecules themselves, not to mention the prevalent processes on a given titania surface. Equations 1-9 only show the initial processes of aqueous phase degradations without going into any detail about the degradation of the chemicals themselves. By looking at the early products of degradation, and thus the early reaction steps, mechanistic insight can be gained, which can help lead to a greater understanding of how to improve the efficiency of the catalysts as a whole. The rest of this thesis describes work in pursuing these chemical concerns.
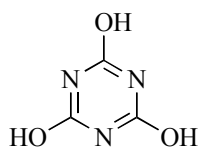
Figure 2. Cyanuric acid

1.5. References

(1)   Lorch, W. *Handbook of Water Purification*; Second ed.; Ellis Horword: Chichester, 1987.

(2)   Management, O. o. W. W.; United States Environmental Protection
Agency: 1998.

(3)   Hoffmann, M. R.; Martin, S. T.; Choi, W.; Bahnemann, D. W. *Chem. Rev.*
1995, *95*, 69-96.

(4)   Huling, S. G.; Pivetz, B. E.; United States Environmental Protection
Agency: 2006.

(5)   Legrini, O.; Oliveros, E.; Braun, A. M. *Chem. Rev.* **1993**, *93*, 671-698.

(6)   Halmann, M. M. *Photodegradation of Water Pollutants*; CRC Press: New
York, 1996.

(7)   Linsebigler, A. L.; Lu, G.; Yates Jr., J. T. *Chem. Rev.* **1995**, *95*, 735-758.

(8)   Fox, M. A. *Chem. Rev.* **1993**, *93*, 341-357.

(9)   Oppenländer, T. *Photochemical Purification of Water and Air*; Wiley-
VCH: London, 2003.

(10)   Murakami, Y.; Kenji, E.; Nosaka, A. Y.; Nosaka, Y. *J. Phys. Chem. B*
2006, *108*, 8751-8755.

(11)   Turro, N. J. *Modern Molecular Photochemistry*; University Science
Books: Sausalito, California, 1991.

(12)   O'Regan, B.; Grätzel, M. *Nature* **1991**, *353*, 737-740.

(13)   Thompson, T. L.; Yates, J. T. *Chem. Rev.* **2006**, *106*, 4428-4453.

(14)   Isley, S. L.; Penn, R. L. *J. Phys. Chem. B* **2006**, *110*, 15134-15139.

(15)   Zhang, Z.; Maggard, P. A. *J. Photochem. Photobiol. A* **2007**, *186*, 8-13.

(16)   Bakaev, V. A.; Steele, W. A. *Langmuir* **1992**, *8*, 1372-1378.

(17)   Ghosh, A. K.; Wakim, F. G.; Addiss Jr, R. R. *Phys. Rev.* **1969**, *184*, 979-988.

(18)   Tahiri, H.; Serpone, N.; Le van Mao, R. *J. Photochem. Photobiol. A* **1996**, *93*, 199-203.

(19)   Hurum, D. C.; Gray, K. A. *J. Phys. Chem. B* **2005**, *109*, 977-980.

(20)   Serpone, N.; Lawless, D.; Khairutdinov, R.; Pelizzetti, E. *J. Phys. Chem.* **1995**, *99,* 16655-16661.

(21)   Calza, P.; Pelizzetti, E.; Mogyorósi, K.; Kun, R.; Dékány, I. *Appl. Catal. B* **2007**, *72*, 314-321.

(22)   Zhang, Z.; Wang, C.-C.; Zakaria, R.; Ying, J. Y. *J. Phys. Chem. B* **1998**, *102*, 10871-10878.

(23)   Shiraishi, Y.; Saito, N.; Hirai, T. *J. Am. Chem. Soc.* **2005**, *127*, 12820-12822.

(24)   Emilio, C. A.; Litter, M. I.; Kunst, M.; Bouchard, M.; Colbeauu-Justin, C. *Langmuir* **2006**, *22*, 3606-3613.

(25)   Wu, Q.; Li, D.; Chen, Z.; Fu, X. *Photochem. Photobiol. Sci.* **2006**, *5*, 653-655.

(26)   Song, H.; Jiang, H.; Liu, X.; Meng, G. *J. Photochem. Photobiol. A* **2006**, *181*, 421-428.

(27)   Engweiler, J.; Harf, J.; Balker, A. *J. Catal.* **1995**, *159*, 259-269.

(28)   Do, Y. R.; Lee, W.; Dwight, K.; Wold, A. *J. Solid State Chem.* **1994**, *108*, 198-201.

(29)   Li, X.; Cubbage, J. W.; Tetzlaff, T. A.; Jenks, W. S. *J. Org. Chem.* **1999**, *64*, 8509-8524.

(30)   Li, X.; Cubbage, J. W.; Jenks, W. S. *J. Org. Chem.* **1999**, *64*, 8525-8536.

(31)   Bouquet-Somrani, C.; Finiels, A.; Graffin, P.; Olivé, J.-L. *Appl. Catal. B* **1996**, *8*, 101-106.

(32)   Oh, Y.-C.; Jenks, W. S. *J. Photochem. Photobiol. A* **2004**, *162*, 323-328.

(33)   Watanabe, N.; Horikoshi, S.; Hidaka, H.; Serpone, N. *J. Photochem. Photobiol. A* **2005**, *174*, 229-238.

CHAPTER 2

Particle size effects on the mechanism and kinetics of degradation of organic molecules using titanium dioxide photocatalysis

2.1. Abstract

Nanometer-size titania photocatalysts exhibit interesting variations in chemical properties due to quantum effects on the semiconductor band gap and, as the particles get slightly larger, due to surface and crystalline properties. Degradation of organic molecules appears to be most efficient at particle sizes between 10 and 100 nm for anatase phase catalysts. This study focuses on the early chemical steps of degradation and degradation kinetics of two probe molecules, 4-methoxyresorcinol (MRC) and 1-*para*-anisyl-1-neopentanol (ANP) when the Millennium PC series anatase titania catalysts are used as the photocatalyst. These catalysts differ in particle size based on the amount of thermal annealing. Degussa P25, a mixed phase catalysts from another source, is used as a standard for high degradation efficiency. Product formation ratios are used to determine the extent of competing oxidative pathways between each catalyst. Multiple chemical probes are employed based on their relative abilities to adsorb to the photocatalyst surface, which changes the oxidation pathways open to them.

2.2. Introduction

Titanium dioxide has been given considerable attention due to its exceptional ability to degrade organic molecules having a multitude of functionalities. In optimizing the conditions for degradation, it has been shown multiple times that the recombination of the two charge carriers, electrons (e^-) and holes (h^+), is the major cause of low degradation efficiency in titania.[1] Many possible solutions to this challenge have been investigated, including main group and metal doping of the catalyst, mixing titania phases, and thermal annealing to induce crystallinity.[1-3]

The particle size, and thus surface area, of the catalyst directly relates to the degree of thermal annealing applied. In smaller particles (1-10 nm), the surface area is quite large; thus organic molecules have more active sites to adsorb to, but surface recombination is also greater, as the charge carriers have less distance to move to recombine. At these sizes, quantum effects lead to a hypsochromic shift in absorbance which allows less sunlight to be used by the catalyst.[4] By thermally annealing these smaller particles, larger particle sizes (>50 nm) can be achieved. Sintering the nanoparticles introduces "deep" electron-trapping sites in the bulk structure[5] and removes detrimental defect sites on the surface by increasing crystallinity.[6] Both of these changes have the effect of reducing charge carrier recombination on the titania surface, which increases the lifetime of the photogenerated hole and allows for more useful chemistry.

However, as particle size increases, the surface area available for excited holes to interact with the solution decreases. This implies that a balance must be struck and that an optimum particle size must be obtained. Many groups have studied this from a

spectroscopic sense, or for efficiency of removal of a particular model compound, and particle sizes from 4 to 75 nm have been implicated as ideal.[6,7] The limit of most of these studies is that they fail to take into account the molecules being degraded and the pathways by which that happens. Two recent studies compare the degradation kinetics of phenol, anisole, pyridine, and other molecules known for selective types of reactivity.[6,8] Their results suggest that the most sintered nanoparticle (75 nm) yields the highest degradation rate for all of the studied molecule. Unfortunately no direct chemical product studies were included in these studies.

Product formation data has the advantage of giving evidence for the primary operating mechanisms on a titania surface, which can't be gained from degradation kinetics alone. In particular, the competition between the direct hole oxidation of an organic substrate and the chemistry associated with the adsorbed hydroxyl radical ($HO^{\bullet}_{ads}$) can lead to very different product distributions based on the substrate employed.

The object of this study is to move towards a deeper understanding of the mechanism of degradation in order to shed light on the optimum nanoparticle size of titanium dioxide. Product studies and kinetics of 4-methoxyresorcinol (MRC, **1**) and 1-*para*-anisyl-1-neopentanol (ANP, **2**) have been used by our group and others in order to study the favored mechanistic pathways of degradation using TiO_2 photocatalysis.

4MRC, **1**   *p*ANP, **2**
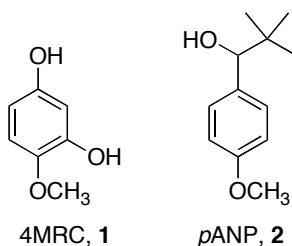
The catalysts in the Millennium PC series all derive from PC 500, which is a 5-10 nanometer catalyst prepared by a sol-gel method. Beginning with the PC 500 catalyst and annealing it to different degrees leads to crystallites with a larger primary particle size. The number designation (i.e. PC 10) is based on the approximate surface area of the catalyst, as shown in Table 1. By using a well-characterized catalyst (P25) and probe molecules that yield reproducible degradation products as a control system, we can compare the PC series catalysts based on their particle size for both kinetic rates and product formation ratios. In this way we can gain insight into the effects of photocatalyst annealing on the mechanisms of early degradation steps previously elucidated for phenolic compounds.

Table 1. Millennium Chemical PC series and Degussa P25 TiO_2

Catalyst	Specific surface area (BET), m^2/g	Average particle size, nm
PC 10	11	75
PC 50	50	25
PC 100	87	20
PC 500	335	8
P25	55	35

2.3. Experimental

All chemicals were obtained from Fisher or Aldrich in the highest purity available and used as received. 4-Methoxyrescorinol was synthesized by a reported method,[9] as was 1-*para*-anisyl-1-neopentanol.[10,11] Degradation intermediates for MRC (Table 3) were obtained commercially or prepared by literature methods.[12] Similarly for ANP (Table 2), compounds **3-5** were obtained commercially. Compound **8** was prepared by a literature method[11] and **6** was prepared by the sodium borohydride reduction of **8**. The same synthetic scheme was used to obtain compounds **6** and **7**. The water employed was purified with a Milli-Q UV plus system resulting in a resistivity ≥ 18 MΩ cm^{-1}. Titania samples employed were PC series from Millennium Chemical and P25 from DeGussa. Table 1 illustrates properties of the PC series as provided by the manufacturer.

The standard suspensions for photocatalytic reactions were prepared at 100 mg TiO$_2$ per 100 mL deionized water (DI water). Sonication for five minutes was used to break up larger aggregates of TiO$_2$. Suspension pH was adjusted to 2.0 (0.01 M HCl), 8.5 (0.1 M NaOH added during the reaction as needed), or 12.0 (0.01 M NaOH). Reactions were also performed at the natural unbuffered pH of the catalyst in water. After an hour of stirring and equilibration in the dark, the desired organic was introduced as a sonicated solution in water at concentrations of 0.3 to 1.0 mM, depending on the substrate. The mixture was then purged with O$_2$ and stirred for 20 minutes in the dark before the irradiation was started. Both stirring and O$_2$ purging were continued throughout the reaction.

Photolyses were carried out with stirring at ambient temperature using a modified Rayonet mini-reactor equipped with a fan and 4-watt broadly-emitting 350 nm "black light" fluorescent tubes. The number of bulbs ranged from two to eight depending on the desired reaction completeness and reaction pH. Ferrioxalate actinomety[13,14] was performed in order to allow semiquantitative comparison of data obtained from reactions with a differing number of bulbs.

In the case of the pH 8.5 reactions, 0.1 M NaOH was added as needed to keep the pH at 8.5 ± 0.5. Reaction times were dependent on the degree of degradation required. Reactions with both probes and P25 taken to high extents of degradation at different pH values were used to gauge the approximate times for <20% degradation of starting material. These times were then used as the basis for all of the PC series reactions.

After the reactions, samples were acidified with Amberlite IR-120 ion exchange resin. The TiO_2 was separated by centrifugation, followed by filtration through a syringe-mounted 0.2 μm PES filter to obtain 1.5 mL aliquots for kinetics or 50 mL samples for product studies. Large samples were concentrated by rotary evaporation to ~ 2 mL and water was then removed by lyophilization.

The dried MRC samples were exhaustively silylated by treatment with 1 mL of anhydrous pyridine, 0.2 mL of 1,1,1,3,3,3-hexamethyldisilazane (HMDS), and 0.1 mL of chlorotrimethylsilane (TMSCl).[15] The resulting mixtures were shaken vigorously for 60 seconds and then allowed to stand for 5 minutes at room temperature. Some precipitate (pyridinium chloride) was separated by centrifugation prior to chromatographic analysis. In the case of ANP, dried samples were dissolved in 500 μL of 0.25 mM dodecane in methanol and directly injected. The partial degradation products were analyzed as their

trimethylsilyl (TMS) derivatives (for MRC) or as is (for ANP) using GC-MS on a Varian star 3400CX Gas Chromatograph using 25 m DB-5 column, coupled with a Finnigan ion trap detector mass spectrometer or an Agilent 6890 GC coupled to a Micromass GCT time-of-flight MS. The temperature program of column was as follows: at 130 ˚C, hold time = 2 min; from 130 to 280 ˚C, rate = 20 ˚C/min. A HP 5890 series II Gas Chromatograph with a 30 m DB-5 or 15 m DB-1 column and an flame ionization detector was also used for routine analysis.

Kinetic data was obtained using HPLC data gathered from 1 mL aliquots that were acidified and centrifuged before injecting into a Varian ProStar or Agilent 1050 liquid chromatograph with a diode array UV/VIS absorption detector. The eluent consisted of a 30:70 mixture of water and acetonitrile (HPLC grade) respectively for ANP, and a 80:20 mixture of 0.2% acetic acid in water and methanol for MRC. The flow rate was set to 1.0 mL/min. A C18 reverse-phase column (Supelco) was used for all probe molecules.

Adsorption equilibria of MRC and ANP on P25 TiO2 were obtained over fixed periods with vigorous magnetic stirring. Solution pH was held at 2.0, 7.0, 8.5, and 12.0 using 10 mM phosphate buffer. Natural pH was also used. Suspensions were prepared from 20 mL buffer containing 50 mg TiO_2. After allowing the desired contact time, an aliquot was removed, centrifuged, and syringe filtered through Millipore filters to remove TiO_2. The residual concentration of compounds was determined by HPLC, with the same conditions as the kinetic studies above. Kinetic study showed that the extent of adsorption reached a constant value after no more than 2 h for both compounds. For the quantitative adsorption experiments, at least 20 h equilibration was allowed before measurement.

2.4. Results and Discussion

The two molecules employed to probe degradations are MRC and ANP. Each of the molecules has been tested in the literature in non-TiO_2 experiments for oxidation by adsorbed hydroxyl radical ($HO^\bullet_{ads}$) and single electron transfer (SET) mechanisms.[12,16] The expected products of both major mechanistic pathways for substituted benzenes have thus been identified. These two molecules have been employed as each has weak interactions that allow for different types of binding with the titania surface. This in turn can lead to different amounts of degradation intermediates resulting from hydroxylation and single electron transfer for each probe molecule.
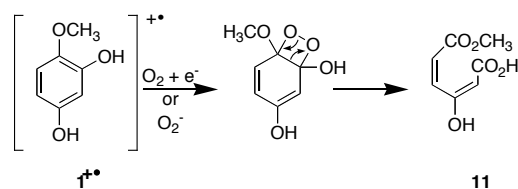
2.4.1. MRC Degradation Products

The intermediates formed upon oxidation of 4-methoxyresorcinol depend both on the catalyst employed and the pH at which the reaction is kept. Based on previous results where Degussa P25 was used, the pH at which the maximum number and concentration of degradation intermediates could be observed was found to be 8.5.[12] For the present work, this pH has been used as both a standard and as a moderately high pH value. Degussa P25 is used as a standard catalyst for titanium dioxide photocatalysis and the major intermediates of MRC degradation using P25 are shown below in Scheme 1, based on past work.[12]
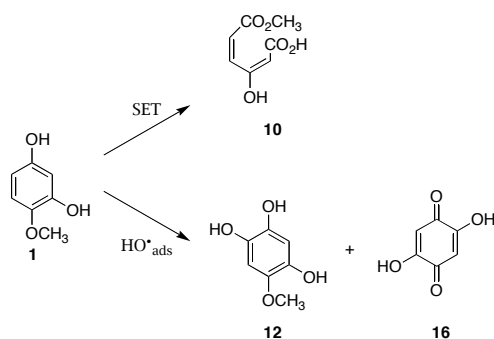
Scheme 1. Major initialproducts of MRC degradation based on photocatalysis with Degussa P25[12]

A brief summary of the degradation mechanisms for MRC is warranted. The SET chemistry of MRC (Scheme 2) involves the formation of a radical cation due to oxidation by a photoexcited hole. This radical is attacked by surface-bound molecular oxygen or superoxide, which then forms a proposed dioxetane that then reopens, breaking the six-membered ring to afford **10**. The chemistry associated with $HO^\bullet_{ads}$ causes hydroxylation of the benzene ring (Scheme 3), which leads to oxygen addition and hydrogen abstraction to form **12**. Another possible mechanism is the abstraction of H• by HO• to make water, and subsequent addition of another hydroxyl radical to produce **12**. The facile oxidation of this molecule in air leads to the benzoquinone product **13** (Table 3), much like in the degradation of 4-chlorophenol.[17]

Once molecules from either path are ring-opened, further oxidations occur to produce C_3 to C_5 molecules that also appear in the product mixture, though usually in smaller amounts. These highly degraded products tell nothing of initial steps of MRC degradation, but presence of these small molecules in absence of **10**, **12**, or **16** implies the formation of the major products, even if early intermediates are quickly degraded.

Scheme 2. MRC ring-opening reaction
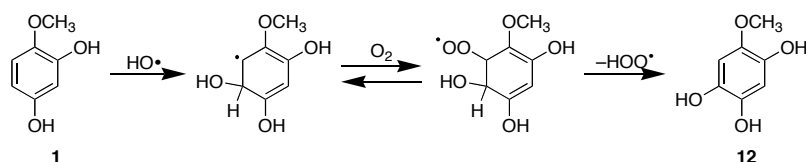
Scheme 3. MRC hydroxylation reaction

2.4.2. ANP Degradation Products

Product formation data was gained from multiple ANP reactions involving P25 and PC series anatase catalysts at different pH. The data in Table 2 show the identified intermediates in the degradation of ANP with retention times and mass spectrometry data for a reaction using P25 at low pH, where the greatest amount of different products appear. High pH reactions and PC series reactions gave fewer products or products in different amounts as mentioned later. Intermediates were verified by comparison to authentic samples with the exception of the proposed product **9**.

The two possible identities of peak **9** are the *ortho*- or *meta*-hydroxylated products. Alkyl hydroxylation products were dismissed due to lack of prior evidence of such products in similar reactions.[18,19] GC-MS data strongly suggests the hydroxyl group is attached to the benzene ring since the M^+ peak is exactly 16 amu higher than ANP (**2**),

and the first two daughter peaks show loss of *tert*-butyl (M$^+$–57), followed by loss of CO (M=28).

Ranchella *et al.*[20] pointed out that both the aldehyde **3** and ketone **8** products are obtained by an SET pathway based on TiO$_2$ photocatalysis studies in acetonitrile that mirror results performed with K$_5$Co^{III}W$_{12}$O$_{40}$,[21] a solution phase electron transfer reagent. Nuclear hydroxylated products, like **6** and **9**, arise from HO$^•_{ads}$ chemistry based on studies with anisole and related benzene derivatives.[17,22] Scheme 4 shows the most probable mechanistic pathway to yield **3**.[20] Although not shown in Scheme 4, the scissed *t*-butyl group is likely attacked by dissolved oxygen and converted to *tert*-butyl hydroperoxide, although it was not investigated. Compound **8**, as mentioned below, is a very minor product, and its formation mechanism in water remains more speculative as it could arise from hydrogen abstraction or from **2$^{+•}$**. The hydroxylation of **2** to **9** is shown in Scheme 5. The formation of **6** involves either an *ipso*-attack by hydroxyl radical on the methoxy position of the phenyl ring or a demethylation reaction, based on related studies of anisole.[22] The final step in Scheme 5 is most likely due to addition/abstraction by molecular oxygen to rearomatize the ring.
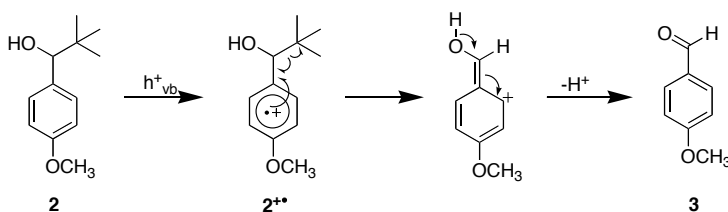
Scheme 4. Mechanism of oxidation of **2** to yield **3**
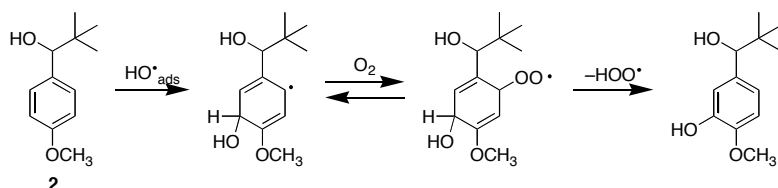
Scheme 5. Mechanism of hydroxylation of ANP to form **9**

Table 2. GC-MS data for ANP products from P25 reactions at low pH[a]

Structure	Formula Weight	Retention Time[b] (min)	Abundance at low pH[c] (low, meduim, high)	MS Peaks: m/z (Relaive Height)
3	136	3.85	low	77 (25), 92 (15), 107 (30), 135 (100), 136 (68)
4	122	4.47	low	65 (23), 93 (38), 121 (100), 122 (91)
5	152	4.96	low	77 (5), 96 (5), 121 (10), 122 (9),135 (12), 151 100), 152 (9)
2	194	5.74	high	65 (3), 77 (15), 109 (25), 121 (10), 137(100), 194 (4)
6	180	6.11	medium	65 (5), 77 (14), 95 (16), 123 (100), 180 (3)
7	178	6.15	low	65 (8), 93 (9), 121 (100), 178 (4)
8	192	6.30	—	77 (18), 91 (19)), 121 (13), 135 (100),192 (1)
9	210	6.86	medium	57 (8), 65 (15), 93 (36), 125 (20), 153 (100), 210 (8)

[a]High pH PC series reactions show fewer products and in different amounts, as mentioned in the text. PC series reactions give the same products in similar ratios
[a]Retention time is based on TOF-MS data.
[b]The relative abundance is compared to the starting material, ANP.

The peak attributed to 4-methoxybenzoic acid (**5**) shows a SET product seen in sensitized oxidations of ANP using organic dyes, but has yet to be seen in titanium dioxide studies.[23] This product is apparently a secondary oxidation product following formation of **3**.[24] In reactions taken up to 50% conversion of ANP, anisole was seen as a very minor product, presumably from a photo-Kolbe reaction of **3**. Compounds **4** and **7** are also secondary products that can be attributed to the further oxidation of **6**, as they appear in only trace amounts in reactions taken to a higher degree of degradation.

The absence of the ketone product **8** from the product mixtures is notable. Ketone **8** is a major product in conventional electron transfer reactions,[23] but is present in only minor amounts in acetonitrile-based titania chemistry.[20] This may be due to direct oxidation of the aromatic ring (Scheme 4) as opposed to direct oxidation of the alcohol or hydrogen abstraction at the benzyl position. Direct oxidation of the ring is favored if close contact to the titania surface is available, which is true in the case aliphatic alcohols, which the benzylic alcohol of ANP can be considered.[25] This aromatic ring attack leads to facile C-C bond cleavage versus C-H cleavage, which is prevalent with *t*-butyl benzyl alcohols and leads to formation of the aldehyde product (Scheme 4).[21] One way to make C-H cleavage more feasible in our system would be to tune ANP by replacing the *t*-butyl group with a methyl, ethyl, or isopropyl group. These groups are less likely to undergo scission and may be competitive with C-H cleavage to form a ketone product, as well as an aldehyde.
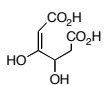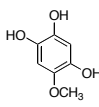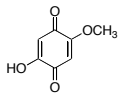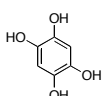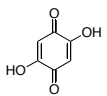
2.4.3. Trends Across the pH Spectrum for MRC Degradation

The effect of pH on titanium dioxide reactions varies depending on the probe molecule being employed, but the trends apply to all of the catalysts studied. At low pH, aliphatic and aromatic acids are known to bind strongly to the surface, which greatly enhances the degradation of these compounds, presumably by facilitating single electron transfer to the catalyst. The acids then undergo a photo-Kolbe decarboxylation on the surface. Successive reactions of this nature lead to complete mineralization.

In the case of benzene derivatives, especially anisoles and phenols, higher pH values have been shown to yield the most efficient degradations.[22] Table 3 shows semiquantitative results for degradation intermediates using PC 100 over the range of pH values employed. Similar results were obtained regardless of the catalyst employed (PC series or P25) as will be discussed below.

At low pH, the rate of degradation and the number and concentration of intermediates formed are both low compared to those at high pH. In the case of pH 2, the only major products observed are those resulting from hydroxylation of the aromatic ring, as shown in Scheme 6. One major product that is formed at low pH is **14**, 1,2,4-trihydroxybenzene. This product is formed by demethylation or by an ipso-attack by $HO^{\bullet}_{ads}$ at the carbon attached to the methoxy group, followed by elimination of methanol. Both mechanisms have been proposed before.[22] Also formed is **12**, which is considered the major hydroxylation product of MRC based on the P25 work.[12] No major SET products are observed, but small amounts of C_3-C_5 products are observed. This indicates that ring-opening must be occurring, and that the major SET product **10** is being further degraded before it can desorb.

Table 3. MRC degradation intermediates from PC 100 reactions as identified by GC-MS.[a]

Structure	Abundance[b] (low, meduim, high)			
	pH 2	pH 5.5	pH 8.5	pH 12
3 (CO$_2$CH$_3$, CO$_2$H, OH)	—	—	low	medium
13 (CO$_2$H, CO$_2$H, HO, OH)	—	—	medium	high
4 (HO, OH, OH, OCH$_3$)	low	medium	high	—
5 (O, OCH$_3$, HO, O)	low	—	low	—
11 (OH, OH, OH)	medium	medium	—	—
12 (OH, HO, OH, OH)	—	—	medium	low
6 (O, OH, HO, O)	—	—	high	high

[a]Similar ratios were obtained for P25 and the rest of the PC series catalysts
[b]Relative to all experiments performed within this study, with the largest abundances being 1-10% that of remaining starting material (by GC integration)

The natural pH of a titanium dioxide reaction is defined as the pH that the natural buffer qualities of TiO$_2$ impose on the system through its own buffer capacity. The natural pH for the PC series was determined to fall between 4.0 and 5.0, with the pH decreasing by ≤1 pH unit within the reaction time. At natural pH, both **12** and **14** are formed in comparable quantity, which is comparable to the pH 2 data.
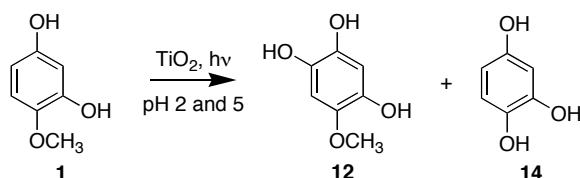
Scheme 6. MRC products at low pH
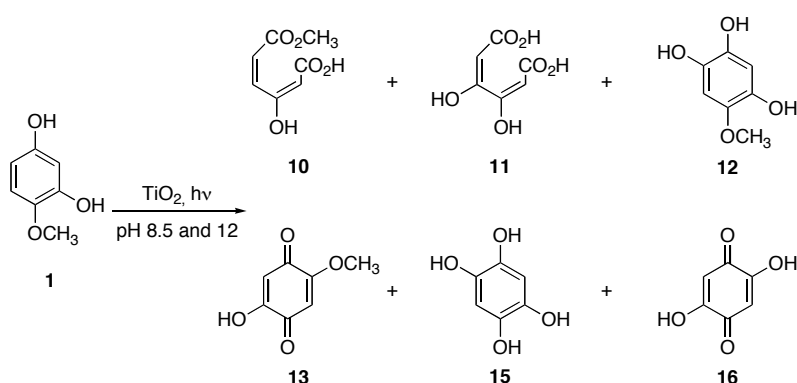

Scheme 7. MRC products at high pH

In the case of pH 8.5, both types of products are present: ring-opening and hydroxylation (Scheme 8). The most prevalent products are **12** and **16,** implying that hydroxyl radical attack is the dominant mechanism. Hydroxylation products **13** and **15** are also present in medium abundance compared to pH 8.5. Unlike the low pH results, **10** and **11** appear in lower quantity compared to the hydroxylated products.

The products at pH 12 offer a complete reversal compared to low pH values. The degradation of MRC is faster at this pH, and the product ratios are much different (Table 3). The major hydroxylation product **12** is not seen at all, nor is the oxidized quinone form. Intermediates **11** and **16** are both present, especially the hydroquinone form **16**,

which is very abundant and second only to **11**. High quantities of **15** and **16** imply that **12** or **14** are being oxidized quickly. Product **11** was not observed in the earlier P25 study of MRC (all of the other products were confirmed with authentic samples), but that may also be due to the reactions not being performed at a higher pH than 8.5. According to GC-MS (ion trap and TOF) of the silylated product mixture, the molecular ion and major daughter peaks are 375, 302, and 257 respectively, which leads to the assignment of the structure shown in Table 3. The difference of 73 between the molecular ion and first daughter are attributed to loss of TMS ($M^{+\bullet}$–73) and the 257 peak is that of a ring opened product with at least five carbons, much like **10**. Although this product must come from both hydroxylation and ring-opening steps, it fits with structures of similar retention times (compared to MRC).
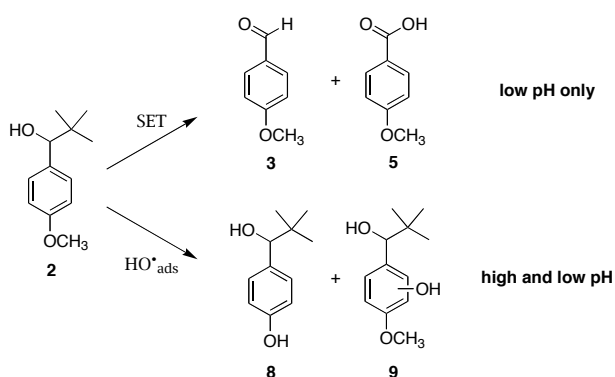
Scheme 8. Major products of ANP degradation based on photocatalysis with Degussa P25 and the PC series.

At low pH, lack of SET products may be due to a lack of interaction between MRC and the TiO$_2$ surface, since this type of chemistry is dependent on a close

interaction between substrate and photocatalyst.[8,25] If MRC can only reach adsorbed hydroxyl radicals in the near-surface and solution phases, SET cannot occur, and the nearby hydroxyl radicals react first to yield products like **12** and **14**. An alternative explanation is that the major SET products are acids, it is also possible that are formed, but bind strongly to the surface and are degrading quickly to products with fewer than six carbons. These C_3 to C_5 products are consistently detected in all MRC reactions, albeit in very small amounts compared to MRC.

As pH increases past ~6, which is the point of zero charge (pzc) for TiO_2, the surface gains an overall negative charge.[2] This negative charge may be able to form hydrogen bonds with MRC, pulling the molecules close to the surface, where SET chemistry can occur, as noted by the appearance of **10** and **11** in the high pH reaction. Since hydroxyl radicals are formed at all pH values, and can be adsorbed to the surface or free in solution, it comes as no surprise that the hydroxylation products are prevalent in the pH range studied.

2.4.4. Trends Across the pH Spectrum for ANP Degradation

The degradation of ANP presents a simpler product mixture (Scheme 4 and Table 3) than that of MRC. Table 3 applies to P25, but much like MRC, the trends for product ratios are the same among all five catalysts studied. At pH 2, ANP degradation affords the appearance of both SET (**3** and **5**) and $HO^{\bullet}_{ads}$ products (**5** and **9**) in nearly equal amounts, though absolute quantification was not attempted. This implies that SET becomes very competitive with hydroxylation at low pH for this molecule. This contrasts with natural pH data that shows hydroxylation products with integrations greater than

10% of the starting material, with SET products making up less than 1%. It should be noted that the latter reaction was taken to slightly higher (~40%) conversion. For example, at higher conversion, if the hydroxylation products are slow to degrade compared to the SET products, then the GC-MS amounts may be misleading, much as in the case of the ring-opened products for MRC.

At high pH, the SET products of ANP are undetectable in the product mixture, whereas the hydroxylation products appear in high abundance, much like in the higher conversion experiment at natural pH mentioned above. The observation of the mechanistic switch to SET with lower pH is special to this molecule due to it having both an anisole and an alcohol group. When these two functionalities are present, albeit as separate molecules in solution, alkanols are known to bind preferentially to the titania surface at low pH values over the aromatic methoxy groups.[26]
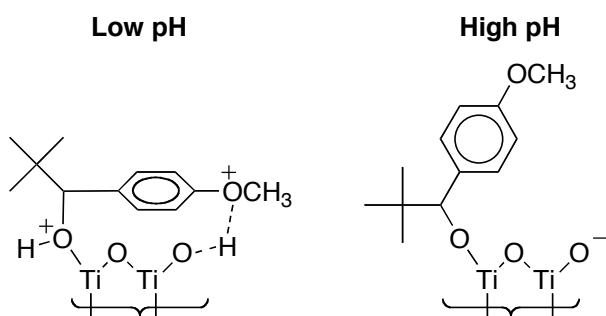
Figure 1. Proposed binding model for ANP

Figure 1 shows an illustration of a proposed binding model for our system, where the alcohol group would bind tightly to the surface, with weak interactions of the aromatic ring and possibly the methoxy group (due to hydrogen bonding interaction).

Adsorption of this nature could produce two results. SET chemistry (oxidation of the side-chain alcohol) would occur to a greater extent at low pH due to the close proximity of the aromatic ring to valence band holes on the surface. Thus the major products of the degradation of ANP at low pH values are aromatic hydroxylation and side-chain carbonyl formation (with small amounts of secondary products involving both SET and HO$^\bullet_{ads}$ mechanisms). At high pH values, the alcoholic binding is still present,[27] but electrostatic repulsion between the negatively charged surface and the methoxy group causes a binding mode change. The new binding motif leaves the aromatic portion situated in the near-surface layers, where only adsorbed and solution phase hydroxyl radicals can reach it. This is true in systems where fluoride displaces weakly bound substrates like phenol.[25]

2.4.5. Comparison of MRC and ANP Degradations

It is interesting to note that the major SET products for each probe molecule appear only at opposite pH values. In the case of ANP, we propose that both the alcohol and methoxy moieties bind to the surface at low pH, allowing for close contact between the aromatic ring and the surface, which is required for SET chemistry.[2] At high pH, the negatively charged surface repels the methoxy group, so that only adsorbed and solution hydroxyl radicals can reach the aromatic ring, quenching direct electron transfer from the surface. pH. Anisole, which is structurally similar to ANP, also displays ring hydroxylation as the predominant reaction in TiO$_2$ photocatalysis.[22] Since MRC contains two hydroxyl groups, it is more susceptible to SET chemistry at higher pH since hydrogen bonding is still possible at pH 8.5 (the pKa's of resorcinol are 9.32 and 9.81).[28]

This implies MRC is capable of weak binding to the titania surface, which allows SET to occur when no competitive binders (like aliphatic alcohols) are present.[12]

The result that neither **10** nor **11** were observed at low pH bears mentioning. Carboxylic acids are known to bind strongly to acidic titania surfaces[2], and studies show that aliphatic alcohols bind competitively.[29] Bound chloride ions (from acidification with HCl) are also competing for surface binding sites,[30] which leaves the anisolic and phenolic groups present on MRC to less specific binding sites or near-surface water layers, where $HO^{\bullet}_{ads}$ is the major reactive species present.[25] Another possibility that warrants investigation is that the low pH mixtures may contain ring-opened products bound to the titania surface. When the samples are worked up, the nanoparticles are removed by filtration, and the bound SET products would then remain with the catalyst in the discarded filter.

The differences in product formations as a function of the PC series catalysts present a striking result. For both probe molecules, the product ratios are the same for every catalyst in the series, and match the product ratios obtained with P25 as a control catalyst. It would appear that the amount of sintering has little effect on structure of the reactive centers on the titania surface, at least in terms of the interactions between the surface and adsorbed molecules. Since sintering is known to induce crystallinity and thus decrease defect sites, it can be speculated that the surface defects thought to be the reactive centers are either unaffected by annealing or are not themselves the most reactive sites on the titanium surface with respect to organic substrates. A look at the reaction kinetics is the logical next step, since the different surface areas of the catalysts would imply a difference in surface reactive site availability.
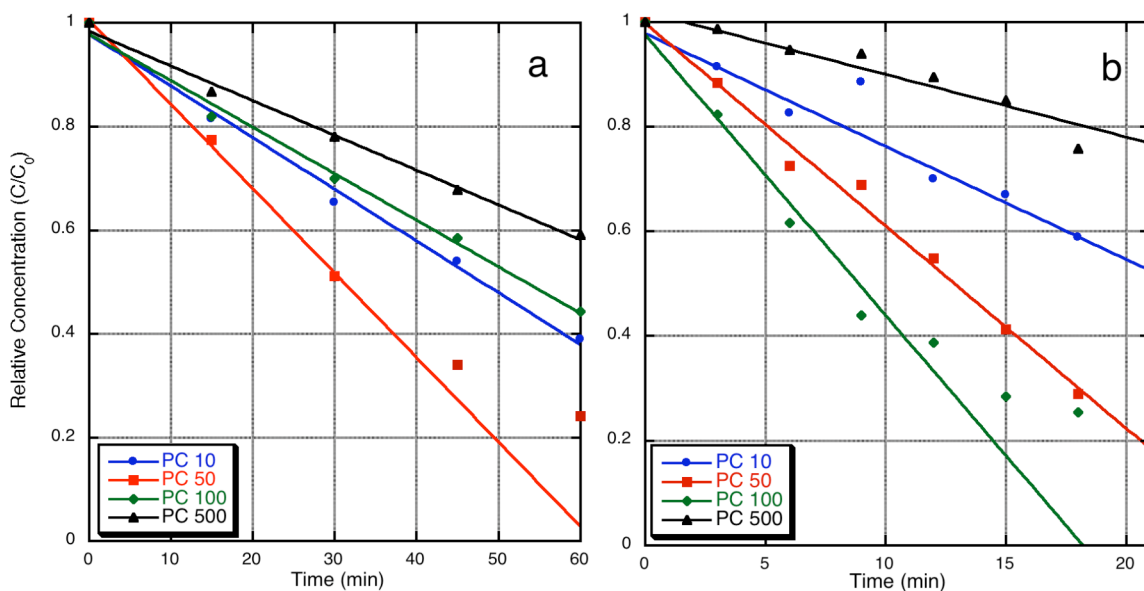
Figure 2. Representative plots of kinetic data a) ANP, pH 12 b) MRC, pH 8.5

2.4.6. Reaction Kinetics

Shown in Figure 2 are representative kinetic plots for MRC and ANP. Table 4 compares the rates of degradation of the two probes over the range of catalysts studied. Organic molecules remediated by titanium dioxide photocatalysis generally follow first-order kinetics when taken to complete degradation. Our interest is not the end products (CO_2, H_2O, etc.), but the initial degradation steps: when the concentration of intermediates is still low and the initial concentration of probe compound is above 80%. In this region, the kinetics can be approximated to zeroth-order, in which the relative rate is simply a linear fit of concentration data (Figure 2). In the case of reactions where the extent of degradation leads to first order kinetics, only the linear portion is used for kinetic data in Table 4. It should be noted that the numbers presented in the table below

depend on the exact experimental conditions of sample geometry, light intensity, etc.

They are appropriated for internal comparisons, but their absolute values are not

especially meaningful. Unless otherwise noted, these kinetic data are calculated as a

function of constant mass of TiO_2, and not as a function of total surface area of TiO_2

used.

Table 4. Rates of degradation of the two probe molecules

ANP[a]	Degradation rate ($\mu M*min^{-1}$)			
catalyst	*pH 2*	*natural pH*	*pH 8.5*	*pH 12*
PC 10	7 ± 1	13 ± 1	9 ± 1	10 ± 1
PC 50	16 ± 1	12 ± 1	14 ± 1	16 ± 1
PC 100	24 ± 1	6 ± 1	11 ± 1	9 ± 1
PC 500	12 ± 1	4 ± 1	5 ± 1	7 ± 1
P25	30 ± 2	30 ± 1	9 ± 1	19 ± 1
MRC[b]				
catalyst	*pH 2[c]*	*natural pH[c]*	*pH 8.5*	*pH 12[d]*
PC 10	1.0	0.6	22 ± 2	
PC 50	1.0	1.0	36 ± 2	
PC 100	0.9	1.1	48 ± 4	
PC 500	0.3	0.04	12 ± 1	
P25	1.2	1.0	28 ± 2	

[a]initial concentration of 2 mM
[b]initial concentration of 0.3 mM, due to low water solubility
[c]performed with 8 bulbs and adjusted using ferrioxalate actinometry(all other are performed with 2 bulbs)
[d]due to rapid base hydrolysis of MRC, kinetic data was not obtained.

2.4.6.1. Kinetic trends over the pH range

It is apparent from Table 4 that the rate of MRC degradation significantly

increases with higher pH. This data shows an order of magnitude drop in rate from pH

8.5 to low pH, which is especially apparent with PC500 where the rate drops from 12 to

0.04 $\mu M*min^{-1}$ as the pH goes below the isoelectronic point of TiO_2. The small amount

of products observed in the low pH reactions fits well with a very low degradation rate, which hardly get above 1 $\mu M*min^{-1}$. Had the low amount of products been due solely to rapid secondary degradation, the rate would not have been affected appreciably, but that is not the case for any of the catalysts. One explanation for this trend could be a consideration of the oxidation potential of MRC as the pH changes. Phenolic compounds with electron donating groups tend to have higher oxidation potentials at low pH and these values decrease with higher pH.[31] Since Table 4 shows a 40 times greater rate of degradation at high pH, it could be that the low pH conditions lead to a coordination sphere around MRC consisting of H-bonded water molecules that disfavor oxidation by h^+_{vb} or $HO^{\bullet}_{ads}$. At high pH when MRC is near its pKa, MRC is oxidized very efficiently, with complete loss of starting material in about two hours. Kinetic data is absent for pH 12 due to a fast base hydrolysis of MRC, which results in a measurable loss of starting material even prior to irradiation.

The trend for ANP shows a moderate increase of rate with decrease of pH, though it is apparent that highly acidic conditions favor degradation, much like carboxylic acids.[32] Since both SET products and hydroxylation appear at low pH, it can be concluded that the increased rate stems partly from increased direct electron transfer from the substrate to the surface, due to tight binding of ANP to the TiO_2 surface at low pH. At high pH, only the hydroxylation mechanism is occurring efficiently, and thus the rate of degradation is decreased due to less specific surface interaction, which results in reaction exclusively with hydroxyl radical (either adsorbed or solution phase).[12]

2.4.6.2. Kinetic trends between titania catalysts

Table 5 shows the same kinetic data as Table 4, only the initial rates have been calculated as a ratio to that of P25 at pH 8.5, which has been used as a standard reaction condition by our group in the past.[17] PC 10 and 50 degrade ANP at nearly the same rate regardless of pH, whereas degradation by the two small catalysts increases by at least a factor of 2 as the pH drops to 2. With the exception of pH 8.5, P25 degrades ANP faster than the PC series over the pH range. This trend does not appear to follow into the MRC degradations, where P25 degrades at a similar rate as the PC series, especially at the two low pH values where almost most of the catalysts degrade MRC at 0.04 $\mu M*min^{-1}$ compared to P25 at pH 8.5.

Table 5. Rates of probe molecule degradation for pH comparison.[a]

	ANP degradation rate ($\mu M*min^{-1}$)				
pH	P25	PC 10	PC 50	PC 100	PC 500
2	3.6±0.3	0.8±0.1	1.9±0.4	2.8±0.2	1.4±0.0
Natural	3.5±0.0	1.5±0.0	1.4±0.0	0.7±0.2	0.4±0.2
8.5	1.0±0.1	1.1±0.2	1.6±0.1	1.3±0.1	0.6±0.1
12	2.2±0.1	1.2±0.1	1.9±0.1	1.1±0.1	0.8±0.0
	MRC degradation rate ($\mu M*min^{-1}$)				
pH	P25	PC 10	PC 50	PC 100	PC 500
2[b]	0.04	0.04	0.04	0.03	0.01
Natural[b]	0.04	0.02	0.04	0.04	0.00
8.5	1.00±0.06	0.80±0.08	1.40±0.06	1.74±0.17	0.43±0.05

[a]Rates are adjusted to P25 pH 8.5 equaling 1.0 $\mu M*min^{-1}$
[b]performed with 8 bulbs and adjusted using ferrioxalate actinometry(all other are performed with 2 bulbs)

Since SET reactions require close association with the surface, a larger surface area would increase the amount of ANP bound to PC 100 and PC 500, which should increase the rate of degradation. SET chemistry makes the majority of pyridine reactivity

with TiO$_2$, and the rate of pyridine removal increases with increased surface area.[6,33] More probe molecules with varied structures would be useful in determining differences between each of the PC series catalysts, for example an aromatic acid that would serve as a strong binding probe that is also susceptible to ring-opening reactions like those of MRC.

Recent results by the Pichat group[6,8] utilizing the PC series show a result not found in our studies. PC 10 degraded pyridine, anisole, and phenol up to ten times faster than any of the other catalysts. Considering the similarity of their latter two probe molecules to MRC and ANP, their result seems out of the ordinary. Without looking at the products formed, it is difficult to speculate about the PC 10 result they obtained. Our study points to PC 50 and PC 100 being the most efficient in terms of degradation kinetics, which makes sense when considering that a balance should be struck between surface area and charge carrier recombination (15-30 nm, based on the particle sizes of PC 50 and 100).

2.4.6.3. Dark adsorption studies

In order to help explain the trends in reactivity for MRC and ANP degradations, dark adsorption studies were carried out. P25 was used as a standard catalyst for all adsorption studies considering its high activity toward MRC and ANP and the similarity of products distributions gathered from it compared to the PC series. The adsorption isotherms in Figure 3 show that the adsorption capacities of ANP and MRC versus equilibrium solution concentration. The maximum adsorption capacities in Table 5 have been estimated as the asymptotic limit of each plot in Figure 3. The adsorption binding

constant, K_{ads}, is characterized by the approach of the adsorption to its asymptotic limit: a faster approach means a larger K_{ads} value. K_{ads} values were estimated using the isotherm data in Figure 3. Each isotherm plot was linearized using the reciprocals of each data point. The binding constants of MRC decrease from 170 to 30 mM^{-1} with increasing pH, with the same trend appearing in adsorption capacity. At high pH, ANP has a binding constant of 8 mM^{-1}. This is an order of magnitude lower than MRC, but the adsorption capacity of ANP is higher than that of MRC at high pH.
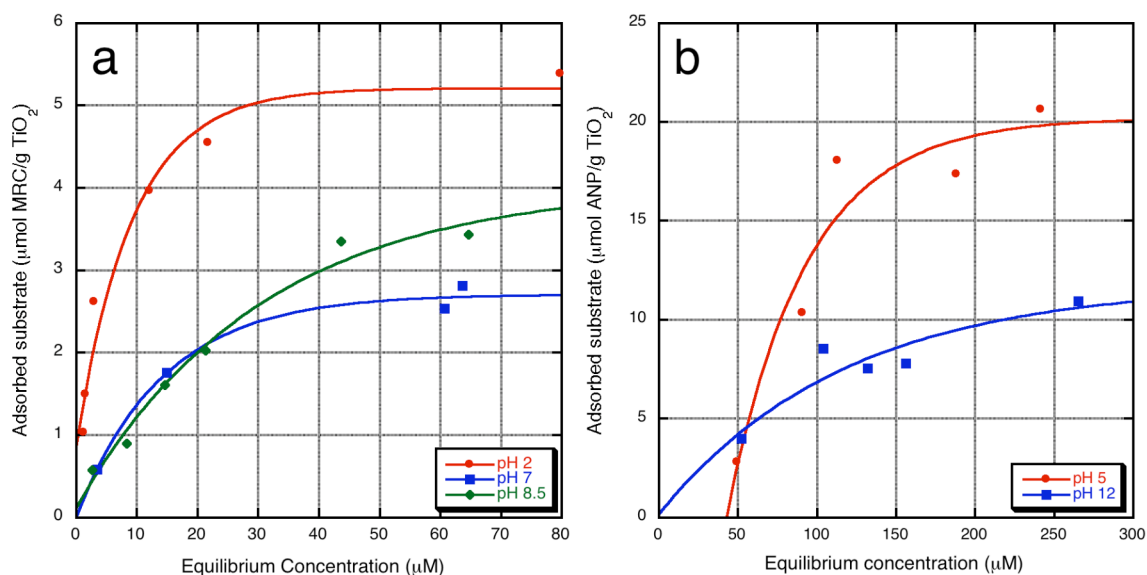
Figure 3. Dark adsorption isotherms for a) MRC and b) ANP. TiO$_2$ catalyst is 2.5 g/L P25 for all cases. Trendlines are exponential rise curves.

Looking at kinetics data (Table 4), it is interesting to note that for MRC, both chemistries (SET and HO$^{\bullet}_{ads}$) are lower by at least an order of magnitude compared to high pH, which implies that more adsorption lowers the reactivity of MRC. In the case of

catechols and benzoic acids, a high binding constant also leads to low degradation, both at low pH and when compared to compounds with less binding affinity (like chlorophenols). This was attributed to the majority of photocatalytic degradation occurring in the surface-solution monolayer or solution multilayers, and not directly on the surface.[34] Thus MRC at high pH degrades fast, since it does not bind as strongly as at low pH. ANP shows a higher adsorption capacity of 10^{-2} mM compared to 10^{-3} mM for MRC but the rates of disappearance of ANP are pH independent (for example PC 50, which has rate constants between 12 and 16 $\mu M \cdot min^{-1}$ over the pH range).

Table 6. Maximum adsorption capacities estimated from dark isotherm plots

Probe molecule	pH	apparent maximum adsorption capacity ($mM \cdot g^{-1}$)	Binding constant (mM^{-1})
MRC	2	5×10^{-3}	170
	7.0	4×10^{-3}	70
	8.5	2×10^{-3}	30
ANP	5	2×10^{-2}	N/A[a]
	12	1×10^{-2}	8

[a]Linearization yields a negative binding constant

Dark adsorption studies between similar benzyl alcohols and phenolic compounds have shown that the general order of binding affinities is ArOH>ArCH₂OH>ArOMe.[26,27] Without the tight binding of a phenolic OH, ANP should not show as striking a contrast in degradation rate between low pH and high pH, which explains the kinetic data. This also leads to ANP having a higher capacity, since less specific binding sites are required for adsorption. This should also carry over to the "rate of adsorption" (K_{ads}) since sites with lower specificity would lead to facile desorption as well as adsorption, which is supported by the high pH values for ANP (8 mM^{-1}) and MRC (30 mM^{-1}).

2.5 Conclusion

Degradation of MRC and ANP using the Millennium PC series has brought some interesting conclusions to light. Under ideal conditions for probe degradation, the most efficient catalysts for starting material removal were PC 50 and PC 100, which would place the ideal particle size between 15 and 30 nm for these catalysts. More appealing is the fact that neither the largest or smallest catalyst provided the most degradation, which would mean that both surface area and charge carrier recombination must be in balance for effective destruction of organic molecules. Also of note is the lack of difference in the mechanisms of degradation between the four PC catalysts, and their similarity to P25 chemistry. This implies that sintering does not affect the active surface species to a great extent since hydroxyl radical and valence-band hole chemistries occur in the same proportions regardless of the catalyst employed. Instead, sintering seems to affect the particle size and surface area such that an optimum efficiency is obtained where surface area and recombination are balanced, which has a direct effect on the rates of probe degradation. To our best knowledge, this is the first direct evidence of this mechanistic effect pertaining to pure titania catalysts. Ongoing research will employ more probe molecules in hopes of expanding this work further.

2.6 References

(1)   Thompson, T. L.; Yates, J. T. *Chem. Rev.* **2006**, *106*, 4428-4453.

(2)   Hoffmann, M. R.; Martin, S. T.; Choi, W.; Bahnemann, D. W. *Chem. Rev.* **1995**, *95*, 69-96.

(3)   Fox, M. A. *Chem. Rev.* **1993**, *93*, 341-357.

(4)   Wang, C.-C.; Zhang, Z.; Ying, J. Y. *Nanostruct. Mater.* **1997**, *9*, 583-586.

(5)   Thompson, T. L.; John T. Yates, J. *J. Phys. Chem. B* **2005**, *109*, 18230-18236.

(6)   Agrios, A. G.; Pichat, P. *J. Photochem. Photobiol. A* **2006**, *180*, 130-135.

(7)   Serpone, N.; Lawless, D.; Khairutdinov, R.; Pelizzetti, E. *J. Phys. Chem.* **1995**, *99*, 16655-16661.

(8)   Enriquez, R.; Agrios, A. G.; Pichat, P. *Catal. Today* **2007**, *120*, 196-202.

(9)   Lang'at-Thoruwa, C.; Song Tong, T.; Hu, J.; Simons Andrean, L.; Murphy Patricia, A. *J. Nat. Prod.* **2003**, *66*, 149-51.

(10)   Janssen, C. G. M.; Godefroi, E. F. *J. Org. Chem.* **1984**, *49*, 3600-3603.

(11)   Smyth, T. P.; Corby, B. W. *J. Org. Chem.* **1998**, *63*, 8946-8951.

(12)   Li, X.; Cubbage, J. W.; Jenks, W. S. *J. Photochem. Photobiol. A* **2001**, *143*, 69-85.

(13)   Hatchard, C. G.; Parker, C. A. *Proc. R. Soc. London, Ser. A* **1956**, *235*, 518-536.

(14)   Bowman, W. D.; Demas, J. N. *J. Phys. Chem.* **1976**, *80*, 2434-2435.

(15)   Sweeley, C. C.; Bentley, R.; Makita, M.; Well, W. W. *J. Am. Chem. Soc.* **1963**, *85*, 2497-2507.

(16)   Linsebigler, A. L.; Lu, G.; Yates Jr., J. T. *Chem. Rev.* **1995**, *95*, 735-758.

(17)   Li, X.; Cubbage, J. W.; Tetzlaff, T. A.; Jenks, W. S. *J. Org. Chem.* **1999**, *64*, 8509-8524.

(18)   Cunningham, J.; Hodnett, B. K. *J. Chem. Soc., Faraday Trans. 1* **1981**, *77*, 2777-2801.

(19)   Papaconstantinou, E. *Chem. Soc. Rev.* **1989**, *18*, 1-31.

(20)   Ranchella, M.; Rol, C.; Sebastiani, G. V. *J. Chem. Soc., Perkin Trans.* **2000**, *2*, 311-315.

(21)   Baciocchi, E.; Bietti, M.; Lanzalunga, O. *Acc. Chem. Res.* **2000**, *33*, 243-251.

(22)   Li, X.; Jenks, W. S. *J. Am. Chem. Soc.* **2000**, *122*, 11864-11870.

(23)   Lykakis, I. N.; Tanielian, C.; Orfanopoulos, M. *Org. Lett.* **2003**, *5*, 2875-2878.

(24)   Mohamed, O. S.; Gaber, E.-A. M.; Adbel-Wahab, A. A. *J. Photochem. Photobiol. A* **2002**, *148*, 205-210.

(25)   Minero, C.; Mariella, G.; Maurino, V.; Vione, D.; Pelizzetti, E. *Langmuir* **2000**, *16*, 8964-8972.

(26)   Bettoni, M.; Del Giacco, T.; Rol, C.; Sebastiani, G. V. *J. Chem. Res., Synop.* **2003**, 415-417.

(27)   Cunningham, J.; Al-Sayyed, G.; Srijaranai, S. In *Aquatic and Surface Photochemistry*; Helz, G. R., Zepp, R. G., Crosby, D. G., Eds.; Lewis Publishers: Boca Raton, 1994, p 317-348.

(28)   Hahn, S.; Kielhorn, J.; Koppenhöfer, J.; Wibbertmann, A.; Mangelsdorf, I. *Resorcinol*, World Health Organization, 2006.

(29)   Sun, Y.; Pignatello, J. J. *Environ. Sci. Technol.* **1995**, *29.*

(30)   Wang, K.-H.; Hsieh, Y.-H.; Wu, C.-H.; Chang, C.-Y. *Chemosphere* **2000**, *40*, 389-394.

(31)   Harriman, A. *J. Phys. Chem.* **1987**, *91*, 6102-4.

(32)   Kesselman, J. M.; Weres, O.; Lewis, N. S.; Hoffmann, M. R. *J. Phys. Chem. B* **1997**, *101*, 2637-2643.

(33)   Cermenati, L.; Pichat, P.; Guillard, C.; Albini, A. *J. Phys. Chem. B* **1997**, *101*, 2650-2658.

(34)   Cunningham, J.; Al-Sayyed, G.; Sedlak, P.; Caffrey, J. *Catal. Today* **1999**, *53*, 145-158.

CHAPTER 3

General conclusions

3.1. Conclusions

The photocatalytic degradation of organic molecules using titanium dioxide was investigated in this work. More specifically, the mechanisms of oxidation occurring on or near the titanium dioxide surface were studied based on results gained by using well-characterized probe molecules whose oxidation products could be attributed to different types of chemistry (SET or hydroxylation). By this method, different titania catalysts can be evaluated based not only on their degradation efficiency, but also on what types of degradation are occurring on the surface.

With our group's previous work in this area, we looked at a series of titanium dioxide catalysts that differ based on their primary particle size.[1-3] The Millennium PC series catalysts are all synthesized as 5 nm (PC 500) catalysts that are then sintered to different degrees to yield 20 nm (PC 100), 25 nm (PC 50), and 75 nm (PC 10) catalysts. Using *para*-anisylneopentanol (ANP) and 4-methoxyresorcinol (MRC) as probe molecules, we found that the particle size has an notable effect on the kinetics of degradation, where PC 50 and PC 100 showed up to a five-fold rate increase compared to the other two catalysts. This has been attributed to two factors. First, these catalysts have sufficiently high surface areas to allow the most favorable interaction with probe molecules. Second, PC 50 and PC 100 seem to have a low enough surface-to-bulk area

ratio to decrease charge carrier recombination on the surface, which is a primary factor in decreasing degradation efficiency of small particles. Looking at the degradation products, the results show no significant difference between the four PC series catalysts with respect to the product ratios at each pH value. This implies that changes induced by sintering on the particle surface of titanium dioxide have little effect on the charge carrier dynamics with respect to their interaction with these probe molecules. In other words, the major effects of sintering on the photcatalyst surface are surface area effects and not the concentration or type of surface reactive sites, otherwise the product formation ratios should differ with pH and particle size. It would be interesting to extend this study to strongly binding molecules that degrade mainly through SET chemistry (like a carboxylic acid) and thus require close surface interaction for any degradation to occur.

3.2. References

(1)   Li, X.; Cubbage, J. W.; Jenks, W. S. *J. Org. Chem.* **1999**, *64*, 8525-8536.

(2)   Li, X.; Cubbage, J. W.; Jenks, W. S. *J. Photochem. Photobiol. A* **2001**, *143*, 69-85.

(3)   Li, X.; Cubbage, J. W.; Tetzlaff, T. A.; Jenks, W. S. *J. Org. Chem.* **1999**, *64*, 8509-8524.